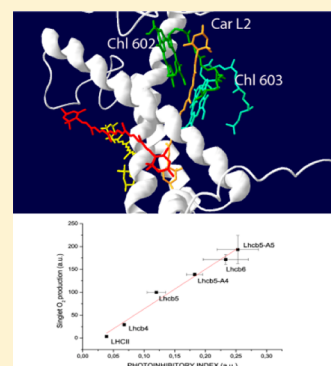


# Chlorophyll Triplet Quenching and Photoprotection in the Higher Plant Monomeric Antenna Protein Lhcb5

Matteo Ballottari,<sup>†</sup> Milena Mozzo,<sup>‡,§</sup> Julien Girardon,<sup>†</sup> Rainer Hienerwadel,<sup>‡</sup> and Roberto Bassi<sup>\*,†</sup><sup>†</sup>Dipartimento di Biotecnologie, Università di Verona, Ca' Vignal 1, strada le Grazie 15, I-37134 Verona, Italy<sup>‡</sup>Laboratoire de Génétique et Biophysique des Plantes, IBEB-SBVME/UMR7265 CNRS-CEA-Université Aix-Marseille, 163 Avenue de Luminy, 13009 Marseille, France<sup>§</sup>Department of Biophysical Chemistry, Groningen Biomolecular Sciences and Biotechnology Institute, University of Groningen, Nijenborgh 4, 9747AG, Groningen, The Netherlands

## S Supporting Information

**ABSTRACT:** In oxygenic photosynthetic organisms, chlorophyll triplets are harmful excited states readily reacting with molecular oxygen to yield the reactive oxygen species (ROS) singlet oxygen. Carotenoids have a photoprotective role in photosynthetic membranes by preventing photooxidative damage through quenching of chlorophyll singlets and triplets. In this work we used mutation analysis to investigate the architecture of chlorophyll triplet quenching sites within Lhcb5, a monomeric antenna protein of Photosystem II. The carotenoid and chlorophyll triplet formation as well as the production of ROS molecules were studied in a family of recombinant Lhcb5 proteins either with WT sequence, mutated into individual chlorophyll binding residues or refolded in vitro to bind different xanthophyll complements. We observed a site-specific effect in the efficiency of chlorophyll–carotenoid triplet–triplet energy transfer. Thus chlorophyll (Chl) 602 and 603 appear to be particularly important for triplet–triplet energy transfer to the xanthophyll bound into site L2. Surprisingly, mutation on Chl 612, the chlorophyll with the lower energy associated and in close contact with lutein in site L1, had no effect on quenching chlorophyll triplet excited states. Finally, we present evidence for an indirect role of neoxanthin in chlorophyll triplet quenching and show that quenching of both singlet and triplet states is necessary for minimizing singlet oxygen formation.



## INTRODUCTION

Oxygenic photosynthetic organisms convert light into chemical energy for CO<sub>2</sub> fixation. In the chloroplast thylakoid membrane the photosynthetic machinery includes two pigment-binding complexes called photosystem I and II (PSI, PSII), together with cytochrome b<sub>6</sub>/f complex and ATPase. Light harvesting is performed by chlorophylls and carotenoids mainly bound to peripheral antenna proteins, called respectively Lhca for PSI and Lhcb for PSII. Here, primary events of light harvesting and excitation energy migration toward reaction centers occur. Being the chloroplast the site of O<sub>2</sub> production, the long-living chlorophyll triplet excited states (<sup>3</sup>Chl\*) produced from singlet excited states (<sup>1</sup>Chl\*) by intersystem crossing easily react to form singlet oxygen and other reactive radical forms (ROS, reactive oxygen species), damaging cell structures.<sup>1–3</sup> This process limits the productivity of plants, and the photosynthetic apparatus is tuned in the different organisms to reduce as much as possible the formation of ROS.<sup>1,3,4</sup> This is achieved by regulating light harvesting and photosynthetic efficiency.<sup>1,5</sup> The <sup>1</sup>Chl\* concentration in the PSII antenna is modulated by nonradiative dissipation activated when light exceeds downstream metabolic activity, with particular reference to the hydrolysis rate of ATP.<sup>6</sup> This process called NPQ (non-photochemical quenching) is localized in the antenna moiety of PSII supercomplexes and needs low luminal pH and the

proton-reactive PSBS subunit for activation in higher plants,<sup>7</sup> while a different protein, called LhcSR, is required in microalgae.<sup>8</sup> Specific xanthophylls, zeaxanthin and lutein, are also required for NPQ activity.<sup>9–12</sup> Although NPQ can dissipate most energy, absorbed photons may still be in excess with respect to photochemical quenching rate, allowing ROS formation by singlet oxygen production.<sup>1,13–15</sup> <sup>3</sup>Chl\* formation occurs mainly at the level of PSII reaction center and Lhcb proteins<sup>16</sup> where xanthophylls act in quenching <sup>3</sup>Chl\* and in scavenging ROS eventually produced. Both of these reactions include formation of carotenoid triplet excited states (<sup>3</sup>Car\*) thermally decaying to ground states in few microseconds.<sup>14,15</sup> Quenching <sup>3</sup>Chl\* by carotenoids occurs via a Dexter mechanism,<sup>17</sup> implying close interactions between donor and acceptor. It has recently been suggested that the sharing of the triplet wave function has a role in favoring fast triplet triplet energy transfer in plant antenna proteins,<sup>18</sup> further supporting the critical role of close chlorophyll to carotenoid interaction for triplets quenching. A special feature of isolated Lhc proteins

**Special Issue:** Rienk van Grondelle Festschrift

**Received:** March 26, 2013

**Revised:** June 20, 2013

**Published:** June 20, 2013

is the inhomogeneous triplet quenching causing a fraction of unquenched  $^3\text{Chl}^*$ , ranging from 5% in trimeric LHCII to 12% in Lhcb5 and 25% in Lhcb4.<sup>11,19,20</sup> Inspection of available Lhcb protein structures, LHCII and Lhcb4, show that chlorophylls are organized in close proximity of four carotenoids called L1, L2, N1, and, in LHCII only, V1.<sup>21,22</sup> L1 and L2 are located at the core of the protein hydrophobic domain with L1 binding lutein and L2 accommodating lutein in LHCII or lutein/violaxanthin/zeaxanthin in monomeric Lhcb4–6 proteins.<sup>10,19</sup> The N1 site, located in between helices A/B cross and helix C, was reported to be specific for neoxanthin and was detected in Lhcb1–5, not in Lhcb6, Lhca, or Lhcsr proteins.<sup>19,23</sup> A fourth carotenoid binding site, called V1, has been reported in trimeric LHCII hosting violaxanthin or zeaxanthin upon activation of xanthophyll cycle.<sup>21,24</sup> Lutein in L1 is in close interaction with chlorophylls 601, 612, and 613, while the xanthophyll in L2 is close to Chls 602, 603, 607, and 609. N1 and V1 carotenoid binding sites are also in close vicinity to Chls 604, 605, 606, 608, and 611, respectively. Reverse genetics has elucidated the specific role of each xanthophyll species in triplet quenching with lutein playing a major role in vivo.<sup>12</sup> Although xanthophylls in L1 and L2 sites are involved in  $^3\text{Chl}^*$  quenching, those in sites N1 and V1 are not.<sup>14,15,19</sup>  $^3\text{Chl}^*$  quenching is also performed by zeaxanthin synthesized by pre-existing violaxanthin in excess light conditions. Interestingly, this activity was reported in monomeric Lhcb proteins especially in Lhcb6 but not in LHCII trimers, confirming the absence of  $^3\text{Car}^*$  formation in V1, where zeaxanthin is located within LHCII.<sup>11,25</sup> In this work we investigated in detail the role of the individual chromophores within a monomeric antenna protein of plant PSII and the relation between  $^3\text{Chl}^*$  quenching and ROS production in Lhcb proteins. We focused on the Lhcb5 complex because of its well-assessed ability of exchanging violaxanthin with zeaxanthin.<sup>9,26</sup> We produced a series of recombinant Lhcb5 holoproteins refolded in vitro in the presence of different xanthophyll species and/or carrying site-specific mutations on residues involved in chlorophyll binding<sup>10</sup> and measured triplet quenching by pump and probe absorption spectroscopy to assess the importance of each chromophore in quenching. Moreover, we measured the rate of ROS production upon illumination. The results allow for a detailed mapping of pigments and Chl-Car interactions involved in efficient  $^3\text{Chl}^*$  quenching in Lhcb5.

## ■ EXPERIMENTAL PROCEDURES

**DNA Cloning, Mutations, Isolation, and in Vitro Refolding of Monomeric Lhcb Proteins.** Lhcb monomeric proteins Lhcb4, Lhcb5, and Lhcb6 were overexpressed in *E. coli* and refolded in vitro as described in ref 26. To improve the quality of in vitro refolding of Lhcb proteins, the absence of trace amounts of degraded, mainly oxidized forms, pigments was checked by high-performance liquid chromatography (HPLC). This was important for obtaining well-folded samples. Site-specific mutations on Lhcb5 were performed as described in ref 10. At least three different preparation for each complex were used for the different analysis herein reported.

**Purification of Trimeric LHCII.** LHCII trimers were purified from *Arabidopsis thaliana* thylakoid membranes as previously described.<sup>24</sup>

**Pigment Analysis.** Pigment binding properties of Lhcb5 complexes were determined by HPLC analysis and fitting of the spectrum of acetone extracts as previously described.<sup>10</sup>

**Fluorescence Measurements.** Fluorescence emission spectra were measured using a Jobin-Yvon Fluoromax 3 spectrofluorimeter. The fluorescence quantum yield was calculated as the ratio between the area below the emission spectra (650–800 nm) upon excitation at 625 nm and the integrated absorption at the excitation wavelength over the 5 nm bandwidth used for excitation.

### Triplet Minus Singlet (TmS) Transient Absorption.

TmS transient absorption measurements were performed as described in ref 19. Samples were diluted to a chlorophyll concentration of 2  $\mu\text{g}/\text{mL}$  in 10 mM HEPES pH 7.5 and 0.03% *n*-dodecyl- $\alpha$ -D-maltoside. Anaerobic conditions were obtained by incubating the sample with 0.02 mg/mL glucose oxidase, 0.04 mg/mL catalase, and 0.02 mg/mL of glucose for 15 min. The excitation wavelength was 640 nm; the kinetics of the absorbance change was recorded at different wavelengths with variable delay times from 5 ns to 5 ms between the actinic and the detection light pulse. A set of measurements with 39 increasing delay times was performed for each kinetic trace. The time between excitations was 300 ms. The kinetics were measured 5–7 times and averaged. Decay kinetics were globally analyzed using Graph-Pad Software. The ms  $^3\text{Chl}^*$  contribution, determined by the decay kinetics, was taken into account as a constant amplitude for the analysis for each wavelength. Chlorophyll to carotenoid triplet–triplet transfer efficiency was calculated as described in refs 14 and 19 as the ratio between the total  $^3\text{Car}^*$  and the sum of the  $^3\text{Car}^*$  and  $^3\text{Chl}^*$  formed: the amount of  $^3\text{Car}^*$  formed was estimated from the positive peak of the  $\mu\text{s}$  component of the TmS decay using as the extinction coefficient the average of  $^3\text{Car}^*$  extinction coefficients ( $\epsilon$ )<sup>27</sup> weighted on the basis of carotenoid composition of the different samples. The amount of  $^3\text{Chl}^*$  formed was estimated from the amplitude of the negative signal of the ms component in the TmS decay using  $\epsilon$  previously reported.<sup>14,19</sup>

**Measurement of Singlet Oxygen Production.** Lhcb samples were diluted at a 2  $\mu\text{g}/\text{mL}$  concentration in a solution containing 0.03%  $\alpha$ -DM, 20 mM Hepes pH 7.5, and 2  $\mu\text{M}$  single oxygen Sensor Green (Invitrogen).<sup>28</sup> Samples were illuminated with red light at 150, 350, and 700  $\mu\text{mol m}^{-2} \text{s}^{-1}$  for 5 min. The concentration of singlet oxygen in solution was detected by measuring the increase in the Sensor Green specific fluorescence at 535 nm, upon 480 nm excitation.

**Photoinhibition Index.** Photoinhibition index for the different complexes was calculated by considering the fluorescence quantum yield and the  $^3\text{Chl}^*$  quenching efficiency. This calculation is aimed at estimating the probability to undergo photoinhibition upon illumination for a Lhcb sample, depending on the concentration of  $^1\text{Chl}^*$  and  $^3\text{Chl}^*$  quenching efficiency. In particular, the photoinhibition index is calculated by multiplying the fraction of unquenched  $^3\text{Chl}^*$  by the fluorescence quantum yield of the same sample, which is indicative of the concentration of  $^1\text{Chl}^*$ .

## ■ RESULTS

**$^3\text{Car}^*$  and  $^3\text{Chl}^*$  Formation in Lhcb5 Reconstituted with Different Carotenoids.** To investigate the role of the different carotenoid species in triplet quenching, we reconstituted Lhcb5 protein in the presence of different xanthophylls as previously reported.<sup>10,29</sup> In particular we reconstituted Lhcb5 with lutein as the only xanthophyll (Lhcb5-L), or with violaxanthin only (Lhcb5-V), lutein and violaxanthin (Lhcb5-LV), lutein, violaxanthin and neoxanthin (Lhcb5-LNV), lutein

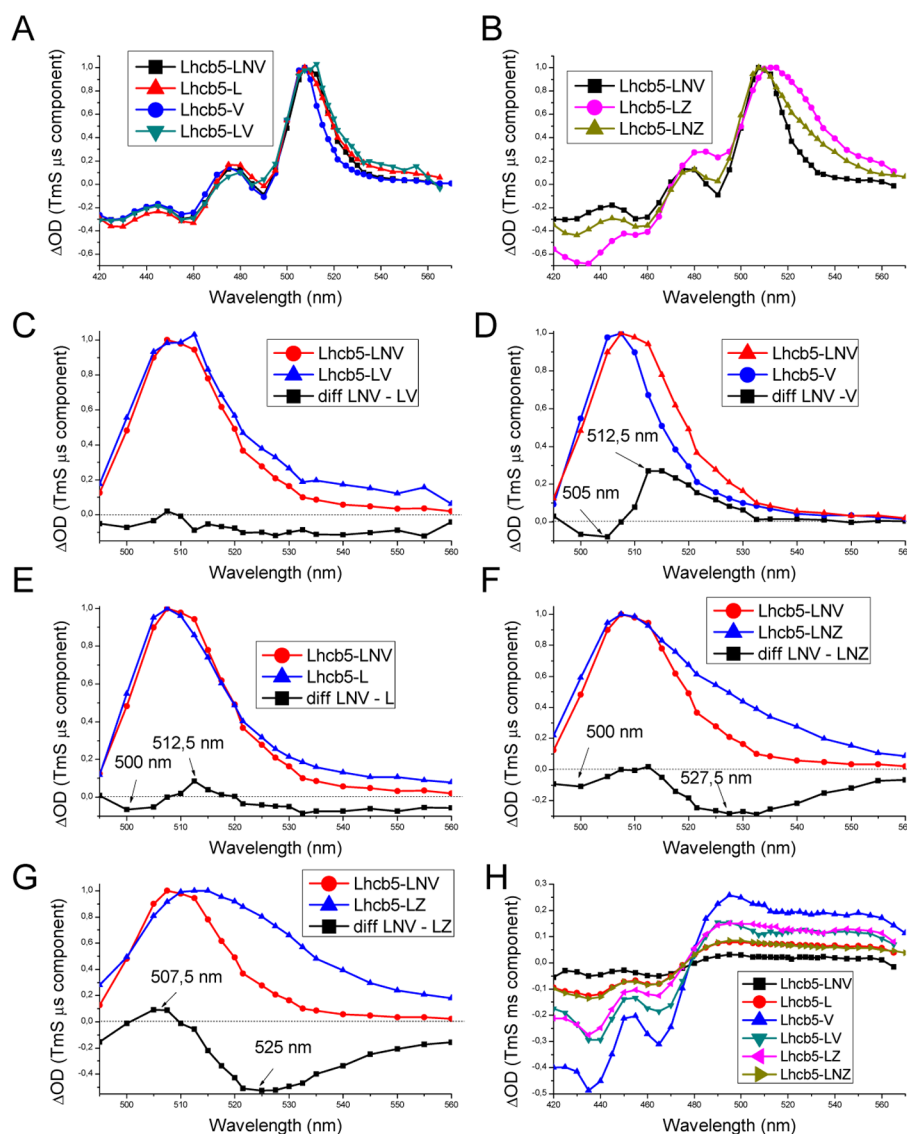


**Figure 1.** Triplets minus singlet (TmS) spectral components of Lhcb5 reconstituted with different carotenoids. Panels A–B:  $\mu s$  decay component ( $^3\text{Car}$ ) associated spectra from TmS decay of Lhcb5 complexes refolded in the presence of different xanthophylls; the spectra were normalized to the peak absorption, and xanthophyll composition is indicated in the legend (L, lutein, V, violaxanthin, N, neoxanthin, Z, zeaxanthin). Panels C–G: Difference spectra obtained subtracting the  $\mu s$  decay component ( $^3\text{Car}$ ) associated spectra from TmS of Lhcb5-LV (C), Lhcb5-V (D), Lhcb5-L (E), Lhcb5-LNZ (F), and Lhcb5-LZ (G) to the  $\mu s$  decay component ( $^3\text{Car}$ ) associated spectra from TmS of Lhcb5-LNV; the wavelengths of difference peaks are reported in the panels. Panel H: ms decay component associated spectra of TmS ( $^3\text{Chl}^*$ ).

and zeaxanthin (Lhcb5-LZ), or lutein, zeaxanthin, and neoxanthin (Lhcb5-LNZ). All of the samples were properly folded as shown by an efficient energy transfer from Chl b to Chl a, detected by steady-state fluorescence measurement with excitation at different wavelengths (data not shown) as reported in ref 10. Pigment composition of the Lhcb5 complexes reconstituted with different xanthophylls is reported in Table S1 (Supporting Information): the different complexes have pigment composition depending on the pigment mix present during reconstitution as previously reported.<sup>10</sup> In particular in all complexes L1 is occupied by lutein, with the exception of Lhcb5-V, which binds violaxanthin in L1.<sup>10,30</sup> L2 is occupied by lutein in Lhcb5-L, by violaxanthin in Lhcb5-V, by a mixture of lutein and violaxanthin in Lhcb5-LV and Lhcb5-LNV, and by lutein and zeaxanthin in Lhcb5-LZ and Lhcb5-LNZ. N1 is occupied by neoxanthin in Lhcb5-LNV and Lhcb5-LNZ, while it remains empty in samples refolded without

neoxanthin.<sup>10</sup> These Lhcb5 holoproteins were analyzed by triplets minus singlets (TmS) time-resolved transient absorption spectroscopy. Briefly, difference absorption kinetics were measured in a pump and probe system with a reference sample kept in the dark vs an identical sample illuminated with strong actinic light to induce triplet formation: absorption of dark samples is due to formation of singlet excited states by chlorophylls and carotenoids, while the signal from the actinic light illuminated sample has an additional transient component due to triplet formation, stimulated by the pump. The decay kinetics of  $\Delta A$ , thus, accounts for triplets decay after pump in the illuminated sample. In anaerobic conditions, where the competing reaction of chlorophyll triplets with oxygen is avoided, the decay of  $\Delta A$  can be fitted by a biexponential function, with a fast component ( $\mu s$ ) related to formation of carotenoid triplets upon  $^3\text{Chl}^*$  quenching, and a slower component (ms) related to residual unquenched  $^3\text{Chl}^*$ .<sup>19</sup> In



Table 1. TmS Fitting Results for Lhcb5 Complexes Analyzed<sup>a</sup>

sample	CHL affected	$\tau$ Car ( $\mu$ s)	<sup>3</sup> Car* max (nm)	<sup>3</sup> Chl* quenching efficiency (%)	<sup>3</sup> Chl* quenching efficiency SD	<sup>3</sup> Chl* unquenched (%)	<sup>3</sup> Chl* unquenched SD
LNV	/	8.80	507.5	87.8%	1.0%	12.2%	2.1%
L	/	8.90	507.5	81.9%	1.0%	18.1%	1.0%
V	/	8.09	507.5	40.8%	4.9%	59.2%	5.8%
LV	/	9.34	512	67.3%	2.6%	32.7%	2.4%
LZ	/	8.35	512.5	79.2%	4.3%	20.8%	3.6%
LNZ	/	8.80	507.5	76.8%	2.5%	16.6%	3.9%
WT	/	8.80	507.5	87.8%	2.1%	12.2%	2.1%
A2	612	8.33	507.5	88.4%	1.4%	11.6%	1.5%
A3	613	8.35	507.5	84.1%	0.4%	15.9%	0.4%
A4	602	8.83	505	81.3%	0.3%	18.7%	0.3%
A5	603	9.07	507.5	79.8%	0.9%	20.2%	0.9%
B3	614	8.96	510	88.3%	0.0%	11.7%	0.0%
B5	609	8.67	507.5	84.0%	0.5%	16.0%	0.5%
B6	606	9.78	510	53.9%	1.7%	46.1%	1.6%

<sup>a</sup>TmS measurements were performed on Lhcb5 complexes refolded in presence of different xanthophylls or mutated on specific chlorophyll binding sites. In the table the chlorophyll affected by mutation is reported, for additional detail see ref 10. Ballottari, M.; Mozzo, M.; Croce, R.; Morosinotto, T.; Bassi, R. Occupancy and functional architecture of the pigment binding sites of photosystem II antenna complex Lhcb5. *J. Biol. Chem.* **2009**, *284* (12), 8103–13. For each complex the decay lifetime of triplet carotenoid is reported, the efficiency of chlorophyll triplets quenching and its standard deviation (SD), and the percentage of triplet chlorophyll unprotected and its standard deviation (SD).

all cases two exponential functions, respectively in the  $\mu$ s and ms time range, were sufficient for satisfactory fitting of the decay curves. The positive bands of the reconstructed TmS difference spectra from the exponential components describe the absorption spectra of <sup>3</sup>Car\* formed upon <sup>3</sup>Chl\* quenching (with lifetimes in  $\mu$ s time range) and the absorption spectra of <sup>3</sup>Chl\*, which remain unquenched in the ms time range. The reconstructed spectra of <sup>3</sup>Car\* formed during the measurement are reported in Figure 1A and B. No major differences could be observed between the spectra from different samples with the exception of Lhcb5-V and zeaxanthin binding complexes (Lhcb5-LZ and Lhcb5-LNZ) in which the major peak in the 510–530 nm spectral range was, respectively, either blue-shifted or red-shifted as compared to those from other complexes (Figure 1). In all samples a single <sup>3</sup>Car\* lifetime was measured around 8.6  $\mu$ s (Table 1), slightly delayed to 8.9 and 9.2  $\mu$ s for zeaxanthin binding complexes (Lhcb5-LNZ and Lhcb5-LZ). <sup>3</sup>Car\* spectra appear to be tuned by the protein environment. In particular it has been reported that <sup>3</sup>Car\* in L1 site are blue-shifted as compared to <sup>3</sup>Car\* in L2.<sup>19</sup> To analyze the formation of <sup>3</sup>Car\* in L1 and L2 binding sites, we subtracted the <sup>3</sup>Car\* spectra of the different sample to the Lhcb5-LNV, considered as a reference (Figure 1, panels C–G). In the case of Lhcb5-LV the difference <sup>3</sup>Car\* spectra (Figure 1C) Lhcb5-LNV minus Lhcb5-LV was not characterized by any defined peak, suggesting a similar <sup>3</sup>Car\* spectrum in the two samples but for some widening in the absence of neoxanthin. Well-defined peaks were only detected in difference spectra between Lhcb5-LNV and the following samples: Lhcb5-V, Lhcb5-L, Lhcb5-LZ, or Lhcb5-LNZ. In particular in the Lhcb5-V minus Lhcb5-LNV difference spectrum (Figure 1D), a positive peak at 512.5 nm and a negative component at 505 nm were evidenced. The different area of these components suggests that both a blue-shift of the <sup>3</sup>Car\* spectrum and lower relative rate of formation of the red-most <sup>3</sup>Car\* component on the overall <sup>3</sup>Car\* occur in Lhcb5-V with respect to the control sample (Lhcb5-LNV). This is likely to be associated with a partially empty L2 carotenoid binding site as suggested by the pigment composition of these samples (Table S1, Supporting

Information). In the case of Lhcb5-L (Figure 1E), the Lhcb5-LNV minus Lhcb5-L difference spectrum is characterized by small positive/negative components at 512.5 and 500 nm, respectively, suggesting a small reduction in the amplitude of the red-most <sup>3</sup>Car\* TmS component. In the case of zeaxanthin binding complexes, Lhcb5-LZ and Lhcb5-LNZ, clear negative components at 527.5 and 525 nm, respectively (Figure 1F–G), are evident in their difference spectra with Lhcb5-LNV, while no significant positive component appears. These negative signals are due to the red-shifted tail appearing in the TmS absorption spectra of Lhcb5-LZ and Lhcb5-LNZ, as previously reported.<sup>27</sup> This result suggests that zeaxanthin accumulation in carotenoid binding site L2 of these samples induces a strong red-shift of the <sup>3</sup>Car\* spectrum,<sup>27</sup> without a major effect on the blue component of <sup>3</sup>Car\*, likely deriving from the carotenoid in L1, where zeaxanthin is not bound. All together, these results show that <sup>3</sup>Car\* spectra can be divided in two forms: the blue-most contribution (peaks at  $\sim$ 500–505 nm) likely depends on xanthophylls in site L1, and is rather insensitive to the xanthophyll species bound therein. The red-most <sup>3</sup>Car\*, in turn, likely derives from carotenoids bound to the L2 site, peaks at 512.5 nm, and is more sensitive to the xanthophyll species hosted with the stronger red-shift being associated to the presence of a zeaxanthin ligand. <sup>3</sup>Chl\* quenching efficiency can be evaluated by comparing the amplitude of the <sup>3</sup>Car\* signal with a  $\mu$ s lifetime, to the overall triplet yield formed, as previously reported.<sup>14,19</sup> To estimate the efficiency of <sup>3</sup>Chl\* quenching by Cars for the different samples, the fraction of the <sup>3</sup>Car\* produced (exhibiting  $\mu$ s lifetime) was divided by the total amount of triplets produced as calculated by summing the amplitude of the <sup>3</sup>Chl\* signal (ms component) and that of the <sup>3</sup>Car\* ( $\mu$ s component) as described in refs 15 and 20. The extinction coefficient used to estimate <sup>3</sup>Car\* concentration were as reported in ref 27. The highest <sup>3</sup>Chl\* quenching efficiency, 88% (implying only 12% of <sup>3</sup>Chl\* remained unquenched), was observed in Lhcb5-LNV, the holoprotein with the composition as found in WT plants grown in control conditions.<sup>31</sup> A slightly lower <sup>3</sup>Chl\* quenching efficiency (82%) was calculated for Lhcb5-L, while binding of violaxanthin in

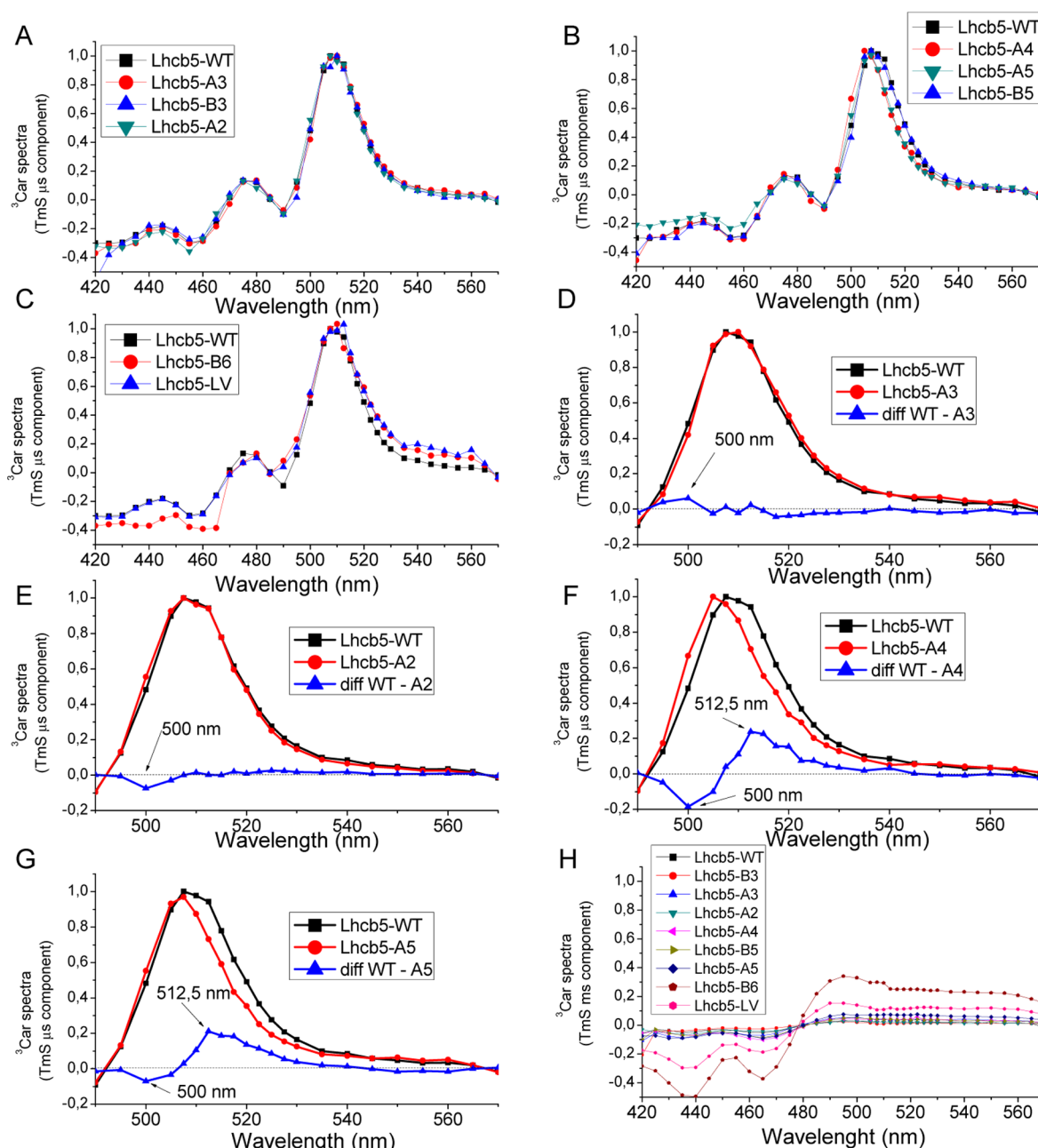


**Figure 2.** TmS spectral components of Lhcb5 WT and mutants. Panel A: Comparison of  $^3\text{Car}^*$  ( $\mu\text{s}$  component of TmS decay) of Lhcb5 WT and mutants on chlorophyll located close to carotenoid binding site L1. Panel B: Comparison of  $^3\text{Car}^*$  spectra of Lhcb5 WT and mutants on chlorophyll located close to carotenoid binding site L2. Panel C: Comparison of  $^3\text{Car}^*$  spectra of Lhcb5-B6 mutant and Lhcb5-WT; since the absence of Chl 606 in mutant B6 induces a loss of neoxanthin, Lhcb5-LV is also reported. Panels D–F: Difference spectra obtained subtracting  $^3\text{Car}^*$  ( $\mu\text{s}$  component of TmS decay) spectra of Lhcb5-A2 (D), Lhcb5-A3 (E), Lhcb5-A4 (F), and Lhcb5-A5 (G) mutants to Lhcb5-WT; significant peaks in the difference spectra are reported. Panel H:  $^3\text{Chl}^*$  spectra (ms component of TmS decay) of Lhcb5-WT and mutants on chlorophyll binding sites;  $^3\text{Chl}^*$  spectra were scaled to the respective  $^3\text{Car}^*$  spectrum. Panel A, B, C, and H have the same Y scale and are comparable.

both L1 and L2 sites (Lhcb5-V) yields the lowest level of  $^3\text{Chl}^*$  quenching (40.8%). Binding of Z in Lhcb5-LZ led to an increase in  $^3\text{Chl}^*$  quenching efficiency with respect to Lhcb5-LV. This effect, however, was not evident when comparing Lhcb5-LNZ to Lhcb5-LNV, which showed a similar efficiency in  $^3\text{Chl}^*$  quenching. It is interesting to note that the level of unquenched  $^3\text{Chl}^*$  was higher in the proteins without neoxanthin. The presence of neoxanthin in N1<sup>21,32</sup> thus increases the efficiency of  $^3\text{Chl}^*$  quenching, yet no additional  $^3\text{Car}^*$  signals beside those from xanthophylls in the L1 and L2

sites, that could be attributed to neoxanthin quenching activity, were evident.

**$^3\text{Chl}^*$  Formation in Lhcb5 Mutants on Chlorophyll Binding Sites.**  $^3\text{Chl}^*$  quenching by carotenoid requires a close distance among chlorophylls and carotenoids, since triplet transfer occurs via Dexter mechanism.<sup>17</sup> Calculations on LH2 complex suggested that the distance should be no larger than 4 Å<sup>33</sup> for efficient triplet transfer. This implies that chlorophylls with closest distance from carotenoid likely have a key role in overall  $^3\text{Chl}^*$  quenching as previously suggested,<sup>19,34</sup> although orientation factors may also be important. To assess whether

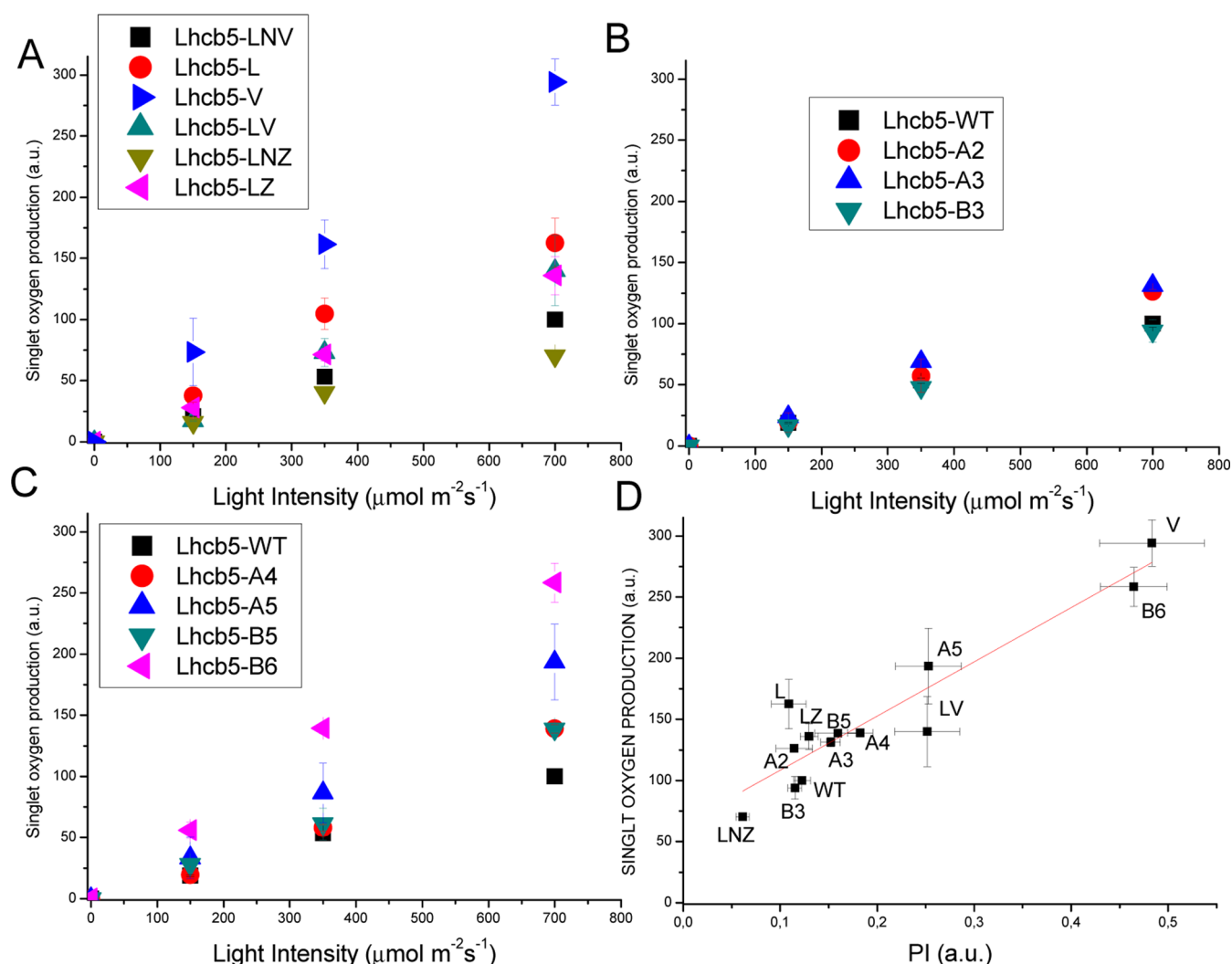


**Figure 3.** Singlet oxygen production of Lhcb5 complexes. Singlet oxygen production of Lhcb5 complexes measured at 150–350–700  $\mu\text{mol m}^{-2} \text{s}^{-1}$  as the increase of 535 nm fluorescence of singlet oxygen Sensor Green dye added to Lhcb5 before illumination. Panel A: Singlet oxygen production in Lhcb5 complexes reconstituted with different xanthophylls. Panel B: Comparison of singlet oxygen produced by Lhcb5 –WT and mutants on chlorophylls located close to site L1. Panel C: Comparison of singlet oxygen produced by Lhcb5-WT and mutants on chlorophyll located close to site L2 and N1. Panel D: Linear relationship in Lhcb5 complexes between singlet oxygen produced at 700  $\mu\text{mol m}^{-2} \text{s}^{-1}$  with the photoinhibitory index (PI) measured as  $^3\text{Chl}^*$  quenching efficiency multiplied for the fluorescence quantum yield of the different complexes; the  $R^2$  value for linear fitting in red is 0.86.

chlorophyll ligands in Lhcb5 are equally involved in energy transfer to carotenoids yielding into  $^3\text{Chl}^*$  quenching, we analyzed a series of recombinant Lhcb5 site specific mutants each targeted to a chlorophyll binding site.<sup>10</sup> It is important to point out that, for changes on excitonic structure of Lhcb5 upon mutation on chlorophyll binding sites, the strong dependence of triplet–triplet energy transfer on the Chl–Car distance enables assigning any variation on TmS spectra of Lhcb5 mutants to the absence of the interaction between carotenoids and the mutated Chl binding sites. In particular, we obtained mutants lacking Chl 602 (site A4), 603 (site A5), 606 (site B6), 609 (site B5), 612 (site A2), 613 (site A3), and 614 (site B3).<sup>10,26</sup> In the following, we will refer as mutant A2, the Lhcb5 mutant where the residue coordinating Chl 612 was mutated, and an analogous indexing was used for the other sites. Pigment composition of Lhcb5 WT and mutants is reported in Table S1 (Supporting Information), showing that each mutation led to the loss of one chlorophyll ligand, with the possible exception of mutations at the two closely interacting

sites A4 and A5 which led to the loss of 2 chlorophyll ligands, which, in the case of mutant A5, were suggested to be Chl 603 and Chl 609. In the case of mutant A4 the identity of missing chromophores is likely to be Chl 602 and a second undefined Chl b.<sup>10</sup> Again, all of the samples were well-folded, as judged by fluorescence emission spectra with different wavelengths of excitation, with the exception of mutant B6, in which a small disconnection was evident that we quantified as 20% of the overall chlorophylls bound.<sup>10</sup> Either steady-state absorption and fluorescence spectra of mutants were similar and consistent with the data previously published.<sup>10</sup>  $^3\text{Chl}^*$  quenching properties of Lhcb5 mutants on chlorophyll binding sites were measured by TmS measurements in anaerobic conditions as described in ref 19. Carotenoid triplet lifetimes, obtained by fitting of decay kinetics, are in the range between 8.33 and 9.78  $\mu\text{s}$ , with less than 5% of deviation among the different samples, suggesting that mutations on specific chlorophyll binding residues do not alter the lifetimes of  $^3\text{Car}^*$ .<sup>19</sup> The decay-associated spectra of carotenoids and chlorophylls were

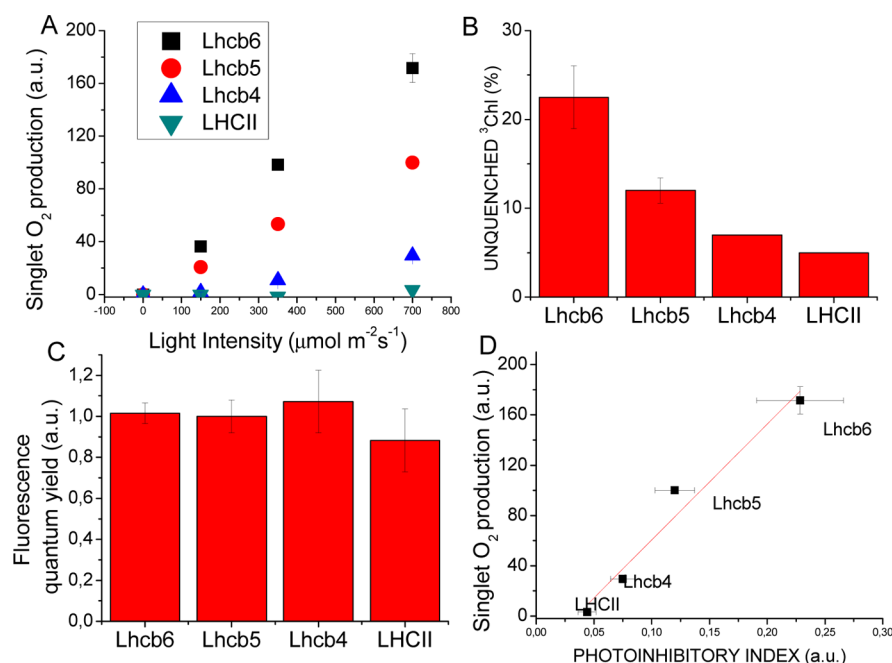


**Figure 4.** Singlet oxygen production,  $^3\text{Chl}^*$  quenching efficiency, fluorescence quantum yield, and photoprotection in Lhcb proteins. Panel A: Singlet oxygen production in Lhcb4, Lhcb5, Lhcb6, and LHCII trimers measured at 150–350–700  $\mu\text{mol m}^{-2} \text{s}^{-1}$  as the increase of 535 nm fluorescence of singlet oxygen sensor green dye added to Lhcb5 before illumination. Panel B: Percentage of triplet chlorophyll unprotected by carotenoid in Lhcb subunits; data for Lhcb4 and Lhcb6 have been measured in this work, and data for Lhcb4 and LHCII were taken from Mozzo et al.<sup>19</sup> Panel C: Fluorescence quantum yield of Lhcb subunits; data are normalized to Lhcb5 value. Panel D: Linear relationship between singlet oxygen produced at 700  $\mu\text{mol m}^{-2} \text{s}^{-1}$  by Lhcb subunits and PI measured as  $^3\text{Chl}^*$  quenching efficiency multiplied for the fluorescence quantum yield of the different complexes; the  $R^2$  value for linear fitting in red is 0.95.

reconstructed from the amplitude of the  $\mu\text{s}$  and  $\text{ms}$  decay components, respectively as described in the previous section (Figure 2). The carotenoid triplet spectra in the 500–580 nm range were characterized by a peak centered at 505–510 nm (Table 1). The  $^3\text{Car}^*$  spectra were thus analyzed by calculating the difference spectra, subtracting the  $^3\text{Car}^*$  component of mutant proteins from the control complex Lhcb5-WT (Figure 2). Mutants on Chls located close to Car binding site L1, A2 (Figure 2D), A3 (Figure 2E), and B3 (Figure S1, Supporting Information) showed an almost identical  $^3\text{Car}^*$  spectrum compared to WT, with a small difference at 500 nm in the case of mutants A2 and A3. A clear blue-shift is evident instead in spectra of mutants A4 and A5. In particular  $^3\text{Car}^*$  spectra of mutants A4 and A5 are characterized by a loss of 512.5 nm component which is fully compensated with an increase of 500 nm contribution in A4 mutant only, while a very small negative component at 500 nm could be observed in the WT minus A5  $^3\text{Car}^*$  spectrum. These results suggest that mutation on A4 and A5 affects  $^3\text{Car}^*$  formation in site L2 by inducing a general blue-shift of  $^3\text{Car}^*$  spectra. It is worth noting that  $^3\text{Car}^*$  spectra of Lhcb5-B6, which was reported to undergo a loss of neoxanthin bound in site N1,<sup>10</sup> and Lhcb5-LV, in which neoxanthin was omitted during the protein folding, are very similar, showing a small but clear widening of the  $^3\text{Car}^*$  major spectral feature (Figure 2C). The  $^3\text{Chl}^*$  quenching efficiency was also unevenly affected by the different mutations (Table 1).

Mutant B6 showed a dramatic decrease of  $^3\text{Chl}^*$  quenching efficiency, leaving up to 46.1%  $^3\text{Chl}^*$  unquenched vs 12.2% in Lhcb5-WT, which can be partially due to the presence of a small fraction of chlorophyll not properly connected in this sample.<sup>10</sup> Mutants on chlorophyll binding sites located close to site L2, for example, A4 and A5 mutants, scored, respectively

18.7% and 20.2% of  $^3\text{Chl}^*$  unquenched, while mutants on chlorophyll binding sites close to L1, for example, A2, A3, and B3, were less affected, scoring respectively 11.6%, 15.9%, and 11.7% of unquenched  $^3\text{Chl}^*$ . This suggests a crucial role of Chl-Car interaction at the L2 site for efficient  $^3\text{Chl}^*$  quenching in Lhcb5.

#### Singlet Oxygen Production in Lhcb5 Complexes.

$^3\text{Chl}^*$  quenching by carotenoids prevents triplet-triplet energy transfer to  $\text{O}_2$  yielding harmful  $^1\text{O}_2$ . To verify whether differences in  $^3\text{Chl}^*$  quenching efficiency were matched by changes in ROS production, we measured the production of  $^1\text{O}_2$  upon exposure to three different light intensities (150–350–700  $\mu\text{mol m}^{-2} \text{s}^{-1}$ ) for 5 min.  $^1\text{O}_2$  produced during the experiment was monitored by the change in fluorescence emission of a dye, singlet oxygen sensor green (SOSG), which increases its 530 nm fluorescence in the presence of  $^1\text{O}_2$ .<sup>27,28,35,36</sup> In Figure 3A the  $^1\text{O}_2$  production of Lhcb5 complexes with different xanthophyll compositions is shown: the Lhcb5-LNZ complex was the sample with the lowest production of  $^1\text{O}_2$  followed by Lhcb5-LNV. Complexes lacking neoxanthin produced more  $^1\text{O}_2$  than those with neoxanthin. Lhcb5-V was the sample with the highest yield in  $^1\text{O}_2$ , followed by Lhcb5-L > Lhcb5-LV > Lhcb5-LZ.  $^1\text{O}_2$  formation in chlorophyll binding site mutants of Lhcb5 is reported in Figure 3B and C. In particular, the production of  $^1\text{O}_2$  is reported for mutants affected on chlorophyll binding sites located in close proximity to the lutein in site L1: mutants A2, A3, and B3 compared to WT (Figure 3B). Mutants A2 and A3 had an increased in  $^1\text{O}_2$  production with respect to WT and mutant B3. In Figure 3C the formation of  $^1\text{O}_2$  is reported for mutants on chlorophyll binding sites located close to carotenoids binding site L2, mutants A4, A5, B5, and/or to N1 site (mutant



B6): all of these mutants had a higher production of  $^1\text{O}_2$  with the mutant B6 showing the highest level, followed by mutant A5. Again, the highest singlet oxygen production in mutant B6 can be attributed to the presence of disconnected chlorophylls unable to transfer to the terminal Chl a emitter. These results suggest a preferential photoprotection of chlorophylls located close to carotenoids binding sites N1 and L2 as compared to chlorophylls located close to site L1. In addition to the rate of triplet quenching by carotenoids, the  $^3\text{Chl}^*$  concentration also depends on the rate of intersystem crossing and, thus, from the concentration of singlet chlorophyll excited states. To integrate these different effects into a functional index, we determined a photoinhibition index (PI) calculated by multiplying the percentage of unquenched  $^3\text{Chl}^*$  by the fluorescence quantum yield of the different complexes (Table S2, Supporting Information). Figure 3D shows the production of  $^1\text{O}_2$  as a function of PI fitted with a linear function: in this plot the values located on top right indicate complexes are more prone to photobleaching (Lhcb5-V, Lhcb5-B6), while values on bottom left indicate more photoprotected complexes (Lhcb5-LNZ, Lhcb5-B3, Lhcb5-WT).

**Singlet Oxygen Production in Lhcb Proteins.** To further investigate the relationship between  $^1\text{Chl}^*$  and  $^3\text{Chl}^*$  quenching ability and the formation of singlet oxygen in other subunits of the PSII antenna system, we extended these measurements to the monomeric Lhcb subunits Lhcb4 and Lhcb6, obtained as previously described.<sup>37</sup> In each case we confirmed that the recombinant proteins refolded in vitro were properly assembled as judged by the high efficiency of energy transfer to Chl a by carotenoids and Chl b.<sup>37</sup> An additional sample, trimeric LHCII, was obtained from *A. thaliana* thylakoids as previously reported.<sup>24</sup> In Figure 4A the dependence of  $^1\text{O}_2$  production on the light intensity is reported for the four samples analyzed, showing the yield of  $^1\text{O}_2$  production was in the following order: Lhcb6 > Lhcb5 > Lhcb4 > LHCII, with LHCII trimers producing a very low amount of  $^1\text{O}_2$ . In Figure 4B the fraction of unquenched  $^3\text{Chl}^*$  of different LHCII proteins is shown.<sup>11,19,20</sup> These values were multiplied by the fluorescence quantum yield of the different Lhcb complexes analyzed (Figure 4C) to calculate the photoinhibitory index (PI). Figure 4D shows that the PI is linearly correlated to the  $^1\text{O}_2$  yield of the individual pigment–proteins, with LHCII appearing as the pigment–protein less susceptible to photo-damage followed by Lhcb4, Lhcb5, and Lhcb6.

## DISCUSSION

We have investigated the role in  $^3\text{Chl}^*$  quenching and photoprotection of the different chlorophyll and carotenoid chromophores within the monomeric Lhcb5 protein. Previous works showed that carotenoids very efficiently (94–97%) quench  $^3\text{Chl}^*$  formed in LHCII trimers.<sup>14,19</sup> In monomeric complexes, this efficiency is reduced, especially in Lhcb5 (88%) and Lhcb6 (~80–70%; Figure 4B). Monomeric Lhc complexes are key subunits in PSII-LHCII supercomplexes, being involved in supercomplex assembly and energy transfer from peripheral antenna to PSII reaction center.<sup>38</sup> Triplet–triplet energy transfer requires a close interaction between chlorophylls and carotenoids in agreement to Dexter's energy transfer model implying that, although excitation energy is delocalized among chlorophylls, mainly Chl a, the removal of a single chlorophyll, thus interrupting Chl–Chl singlet energy transfer, can have a strong impact on the overall Chl–Car triplet–triplet energy transfer. In addition, the conformational changes induced by

binding of xanthophyll's cycle pigments in excess light conditions affect the efficiency of  $^3\text{Chl}^*$  quenching, thus introducing a trade-off between the different functions of antenna proteins including light harvesting, ROS scavenging,  $^1\text{Chl}^*$  quenching, and  $^3\text{Chl}^*$  quenching.

### $^3\text{Car}^*$ Formation in Lhcb5 Carotenoid Binding Sites.

The comparison of Lhcb5 complexes refolded in vitro with different pigment composition allows us to determine the spectroscopic characteristic of  $^3\text{Car}^*$  in Lhcb5. The peak wavelength of singlet and triplet states of carotenoids bound to Lhcb5 is differentially tuned on the base of the local protein environment. Carotenoids bound to sites N1 and V1 appear to be silent as for the formation of  $^3\text{Car}^*$  upon chlorophyll excitation since no significant changes in TmS spectra are evident when comparing samples with or without N1 or V1 occupancy, in agreement with previous observation in LHCII.<sup>14,15,19</sup> We assign the red-most  $^3\text{Car}^*$  absorption contribution to the ligand of site L2 based on its dependence on changes in L2 occupancy (Figure 1), consistent with previous reports,<sup>19,20</sup> and on the results obtained with mutants on chlorophyll binding sites located close to the carotenoid in site L2 (Figure 2). Violaxanthin and zeaxanthin bind to site L2 in minor monomeric Lhcb complexes.<sup>10,11,22,41</sup> Consistently, zeaxanthin induces a red-shift to  $^3\text{Car}^*$  spectrum,<sup>27</sup> Figure 1; violaxanthin instead produces a clear blue shift in  $^3\text{Car}^*$  spectra. The higher Chl/Car ratio in this sample as compared to Lhcb5-LNV complex (Table 1) suggests that in Lhcb5-V L2 site is partially empty. Further support is provided by TmS spectra of Lhcb5 mutants targeting chlorophyll binding sites since deletion of a chlorophyll located in close contact to a specific xanthophyll binding site, where efficient triplet–triplet energy transfer occurs, is expected to reduce the amplitude of  $^3\text{Car}^*$  signal associated to that binding site. Based on the homology model of Lhcb5 based on the X-ray structures of LHCII<sup>21,39,40</sup> and Lhcb4<sup>22</sup> (Figure 5), the chlorophylls which likely contribute to  $^3\text{Car}^*$  formation in site L1 are Chl 610–Chl 612–Chl 613, while contributions to  $^3\text{Car}^*$  formation in site L2 come from Chls 602–603, close to the L2 site.<sup>10,21,22,40</sup> Thus, the red-most component of TmS spectra is significantly reduced produced in mutant A4 (Chl 602) and A5 (Chl 603).

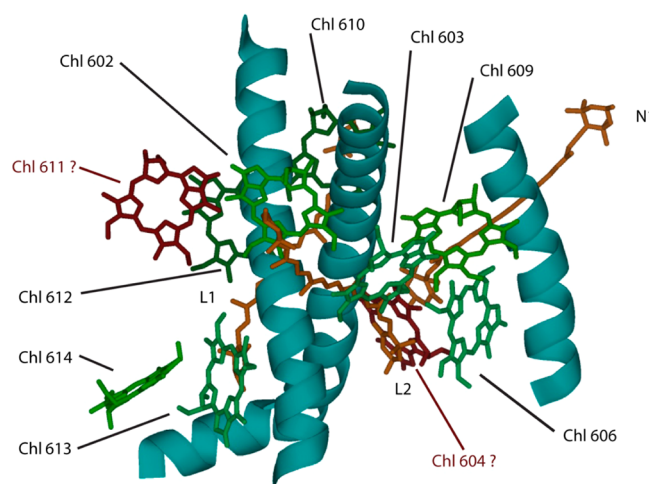


**Figure 5.** Lhcb5 chromophore map. Data from mutational analysis have been employed to build up a Lhcb5 chromophore map. Chl, carotenoids, and  $\alpha$ -helix positions are from LHCII.<sup>21</sup>



**$^3\text{Chl}^*$  Quenching Efficiency.** The efficiency of  $^3\text{Chl}^*$  quenching in Lhcb5 is  $\sim 87.8\%$  in close agreement with a previous report.<sup>19</sup> Surprisingly,  $^3\text{Chl}^*$  quenching efficiency is essentially unaffected in mutant A2, missing Chl 612, the red-most Chl in Lhcb5, located very close to site L1 (less than 4 Å in Lhcb4 and LHCII). This chlorophyll ligand has been proposed to be the major site for Chl-Car triplet-triplet transfer<sup>34</sup> in Lhcb6, where  $^3\text{Chl}^*$  quenching drops to 50% upon deletion of Chl 612.<sup>20</sup> The strong difference in the result of the homologous mutations in Lhcb5 vs Lhcb6 clearly show that in spite of overall homology in these holoproteins chromophore organization can be strikingly different accounting for the conservation of Lhcb1-6 proteins through land plants. Alternatively, the explanation for the different effects of the A2 mutation in Lhcb5 vs Lhcb6 might be found in the heterogeneity of the Lhcb6-A2 mutant protein sample, 50% of which had an empty carotenoid binding site L1 nearby, while the effect of a missing  $^3\text{Chl}^*$  donor or a carotenoid acceptor cannot be distinguished in terms of  $^3\text{Chl}^*$  quenching efficiency. Instead, Lhcb5-A2 analyzed in the present work exhibited full occupancy of site L1. In accordance with our data, previous work on LHCII showed an increased photoprotection efficiency in the absence of Chl 612.<sup>42</sup> Thus, we suggest that Chl 612 has only a minor role, if any, in Chl to lutein triplet transfer in Lhcb5. This is further supported by the observation that the deletion of Chl 612 did not cause an increase of  $^3\text{Chl}^*$  from uncoupled Chl, implying that Chl 612 only contributed to lutein L1 triplets formed by Chl 612 itself rather than bridging for  $^3\text{Chl}^*$  transfer from Chl 611 to Car in L1 as suggested for Lhcb4 and LHCII.<sup>39,43</sup> Our results on A2 mutant do not imply that Chl 612 is not involved at all in  $^3\text{Chl}^*$  quenching, but that in its absence, energy is re-equilibrated among the different chlorophylls, and  $^3\text{Car}^*$  in L1 can be formed probably via Chl 613 or Chl 610, without major loss in  $^3\text{Chl}^*$  quenching efficiency. The role of Chl610 on  $^3\text{Car}^*$  formation cannot be investigated since mutation on its binding residues makes the mutant protein unstable.<sup>10</sup> The mutation at site A3, by causing the loss of Chl 613, significantly reduces  $^3\text{Chl}^*$  quenching efficiency, with  $\sim 16\%$  of  $^3\text{Chl}^*$  unquenched. This result suggests that the interaction between Chl 613 and Chl 614 is needed for quenching  $^3\text{Chl}^*$  614, this Chl being located too far apart from lutein in L1 for direct triplet-triplet energy transfer.<sup>21,34</sup> The coupling between Chl 614 and Chl 613, interacting with carotenoid in L1, is thus necessary and sufficient for  $^3\text{Chl}^*$ 614 quenching. Consistently, mutant B3, missing Chl 614, has a level of unquenched  $^3\text{Chl}^*$  very similar to WT, implying that  $^3\text{Chl}^*$  originated from Chl 614 in the WT are efficiently quenched through Chl 613. The identification of Chl 614 as a possible source for harmful  $^3\text{Chl}^*$ <sup>34</sup> is, however, justified due to its exceeding distance from carotenoid in L1. It is interesting to note that Chl 614 is absent in many Lhcb proteins involved in the response to photo-oxidative stress such as LhcSR3 and Lhcbm1 from *Chlamydomonas reinhardtii* and in both Lhcb4.3 and Lhcb6 from *A. thaliana*, in which the  $^3\text{Chl}^*$  quenching efficiency is generally lower as compared to most Lhc proteins (Figure 4).

The analysis of chlorophyll binding site mutants located close to the carotenoid in L2 clearly demonstrates an important role for Chl 603 and Chl 602 (missing in mutant A5 and mutant A4, respectively), where the level of unprotected  $^3\text{Chl}^*$  was increased to 20.2% and 18.7%, respectively. The Chl 603–602 dimer has been reported to be one of the Chl clusters with the lower transition energy level, similar to Chl 613–614

cluster, slightly higher than Chl610–611–612<sup>44,45</sup> in LHCII. Our results show that Chl 613–614 and Chl 602–603 pairs are important for efficient  $^3\text{Chl}^*$  quenching, far more than the Chl 612–610 cluster. Chl 602–603 pair may also be responsible for receiving excitation energy from Chl 609 and from Chl 606. In fact, it has been suggested that Chl 604 is not present in Lhcb5,<sup>44</sup> thus leaving Chl 606 uncoupled. It is important to note that Chl 606 in B6 binding site is mostly Chl b:<sup>10</sup> since  $^3\text{Chl}^*$  formation takes nanoseconds<sup>14,19</sup> and Chl b > Chl a energy transfer occurs in subpicosecond time scale,<sup>46</sup> Chl 606 is expected to have a very low excited states population since a cluster of Chl a as Chl 602–603–609 is present in the neighbor position. The absence of Chl 606 in mutant B6 induces a strong reduction in  $^3\text{Chl}^*$  quenching: this result is due to the presence of a fraction (23%) of disconnected Chl in this mutant, as previously reported<sup>10</sup> as well as a perturbation of the protein conformation resulting from the loss of neoxanthin in this mutant. The role of neoxanthin in  $^3\text{Chl}^*$  quenching is indeed evident from the observation that all of the complexes refolded in the absence of this xanthophyll have a decrease in  $^3\text{Chl}^*$  quenching efficiency. A similar effect was also reported for LHCII<sup>19</sup> and should be considered to explain the low  $^3\text{Chl}^*$  quenching efficiency in Lhcb6, lacking neoxanthin, compared to other Lhcb proteins which have a neoxanthin ligand. The analysis of Lhcb5 complexes with different xanthophyll complement shows that both neoxanthin and lutein are needed to maximize  $^3\text{Chl}^*$  quenching (Table 1). This is likely due to a loose folding of the pigment–protein complex. Consistently, the thermal stability of the complex is reduced in the absence of neoxanthin<sup>10</sup> (Supporting Information, Table S1), while in the absence of lutein, the L2 site, particularly active in  $^3\text{Chl}^*$  quenching in Lhcb5 (see above), is partially empty (see Lhcb5-V, Supporting Information, Table S1).<sup>10</sup>

The role of zeaxanthin in  $^3\text{Chl}^*$  quenching is complex: Lhcb5-LNZ has a similar or even lower efficiency in  $^3\text{Chl}^*$  quenching as compared to Lhcb5-LNV. This result is consistent with reports on LHCII trimers,<sup>19,27</sup> but in contrast from the case of Lhcb6<sup>11</sup> and Lhcb monomers.<sup>27</sup> By comparing Lhcb5-LV vs Lhcb5-LZ, the presence of zeaxanthin in site L2 clearly leads to an increased  $^3\text{Chl}^*$  quenching efficiency. The same effect was observed in Lhcb6 which also lack neoxanthin. However, zeaxanthin was reported to increase  $^3\text{Chl}^*$  quenching efficiency *in vivo*.<sup>27</sup> This suggests that, although the  $^3\text{Chl}^*$  quenching enhancement effect does not occur in Lhcb5, yet it is important in other Lhc proteins where neoxanthin is not a ligand, such as Lhcb6 and all Lhca proteins. We suggest that the efficiency of  $^3\text{Chl}^*$  quenching in LHCII and Lhcb5 in presence of neoxanthin is controlled by the tightness of pigment–protein assembly. This effect rather than being specifically due to neoxanthin, should be referred to N1 occupancy. In fact the *Arabidopsis* mutant *aba4*, in which neoxanthin is not accumulated, fills the N1 site with violaxanthin.<sup>35</sup> When the N1 site is empty, Lhc proteins are more flexible and prone to leave some  $^3\text{Chl}^*$  unprotected by carotenoid (Figures 3 and 4) as in the case of Lhcb6 or Lhcb5-LV. In these, the conformational changes induced by zeaxanthin binding increases  $^3\text{Chl}^*$  quenching efficiency, possibly by minimizing the chlorophylls to carotenoids distance. This hypothesis is consistent with the observed increase in Chl-Chl interactions upon zeaxanthin binding.<sup>47</sup>

**Quenching of Both Chlorophyll Triplet and Singlet Excited States Contribute to Preventing ROS Formation.** Photoprotection mechanisms in Lhc antenna proteins have

been evolved to prevent ROS formation, in particular  $^1\text{O}_2$ . We show (Figures 3 and 4) an inverse correlation between the rate of  $^1\text{O}_2$  production and neoxanthin abundance. It is relevant to ask what determines the rate of  $^1\text{O}_2$  production. The mutant Lhcb5-A5 is characterized by a very high  $^1\text{O}_2$  production, while the mutant Lhcb5-A4 has an intermediate behavior, despite having a similar  $^3\text{Chl}^*$  quenching efficiency. This result can be interpreted based in Figure 3D. When considering the dependence of  $^1\text{O}_2$  formation on the PI index, which takes into account both triplet and singlet quenching, mutant A5 has a lower capacity for  $^1\text{Chl}^*$  quenching than mutant A4,<sup>10,26</sup> resulting into a higher probability of  $^3\text{Chl}^*$  formation. Indeed, the percentage of  $^3\text{Chl}^*$  unprotected by carotenoids itself is not sufficient to predict the risk of  $^1\text{O}_2$  formation; the probability of  $^3\text{Chl}^*$  production from  $^1\text{Chl}^*$  should also be considered. Here, the latter was estimated by considering the fluorescence quantum yield of the different complexes to be inversely related to quenching efficiency of  $^1\text{Chl}^*$  excited states. The linear correlation between  $^1\text{O}_2$  formation and PI reported in Figures 3D and 4D shows that both  $^1\text{Chl}^*$  and  $^3\text{Chl}^*$  quenching mechanisms cooperate to prevent ROS production. In this context it clearly appears that zeaxanthin has a crucial photoprotective role, since it induces a strong reduction of  $^1\text{Chl}^*$  excited states population and thus a lower probability of  $^3\text{Chl}^*$  formation. Thus, altogether Lhcb5 is less prone to produce  $^1\text{O}_2$  upon zeaxanthin binding despite a slightly lower efficiency in  $^3\text{Chl}^*$  quenching. Finally, zeaxanthin binding also causes a reduction in excitation pressure on PSII reaction center through its  $^1\text{Chl}^*$  quenching effect, thus reducing photo-oxidative stress in PSII RC from charge recombination.

## CONCLUSIONS

In this work we analyzed the managing of  $^3\text{Chl}^*$  in Lhcb5 as dependent on the role of its carotenoid and chlorophyll chromophores. The spectroscopic properties of  $^3\text{Car}^*$  from site L2 are sensitive to xanthophyll occupancy and on the presence of chlorophylls located nearby, as Chl 602 and Chl 603. In particular, we show that the interaction between the Car in site L2 with Chl 602 and Chl 603 is crucial for efficient  $^3\text{Chl}^*$  quenching. Thus,  $^3\text{Car}^*$  formation in site L2 plays an important role in avoiding photoinhibition. We showed that  $^3\text{Chl}^*$  quenching efficiency is unaffected in absence of Chl 612, at difference with results in other members of the Lhc family.<sup>19,20,48</sup> Neoxanthin in N1, although not playing a direct role in  $^3\text{Chl}^*$  quenching, is necessary for efficient photoprotection, likely through a stabilization of the protein conformation and the tightening of Chl-Chl and Chl-Car interactions (Table S1, Supporting Information). Finally, we show that  $^3\text{Chl}^*$  and  $^1\text{Chl}^*$  quenching mechanisms cooperate to prevent ROS formation, explaining the special role of zeaxanthin which improves the photostability of the protein by decreasing  $^1\text{Chl}^*$  population, thus reducing the probability of  $^3\text{Chl}^*$  formation.

## ASSOCIATED CONTENT

### Supporting Information

Table S1: Pigment binding properties of Lhcb5 complexes reconstituted with different xanthophyll and mutated on specific chlorophyll binding sites. Table S2: Fluorescence quantum yield of Lhcb5 complexes. Figure S1: Triplet carotenoid excited states spectra of Lhcb5 WT and mutant

B3, B5, and B6. This material is available free of charge via the Internet at <http://pubs.acs.org>.

## AUTHOR INFORMATION

### Corresponding Author

\*Tel.: +390458027916. Fax: +390458027929. E-mail: roberto.bassi@univr.it.

### Notes

The authors declare no competing financial interest.

## ACKNOWLEDGMENTS

This project was supported by EU project 238017 HARVEST and EU project 316427 ACCLIPHOT.

## REFERENCES

- (1) Niyogi, K. K. Photoprotection Revisited: Genetic and Molecular Approaches. *Annu. Rev. Plant Physiol. Plant Mol. Biol.* **1999**, *50*, 333–359.
- (2) Russell, A. W.; Critchley, C.; Robinson, S. A.; Franklin, L. A.; Seaton, G.; Chow, W. S.; Anderson, J. M.; Osmond, C. B. Photosystem II Regulation and Dynamics of the Chloroplast D1 Protein in Arabidopsis Leaves during Photosynthesis and Photo-inhibition. *Plant Physiol.* **1995**, *107* (3), 943–952.
- (3) Niyogi, K. K.; Björkman, O.; Grossman, A. R. The Roles of Specific Xanthophylls in Photoprotection. *Proc. Natl. Acad. Sci. U.S.A.* **1997**, *94* (25), 14162–7.
- (4) Steffen, K. L.; Wheeler, R. M.; Arora, R.; Palta, J. P.; Tibbitts, T. W. Balancing Photosynthetic Light-Harvesting and Light-Utilization Capacities in Potato Leaf Tissue during Acclimation to Different Growth Temperatures. *Physiol. Plant.* **1995**, *94* (1), 51–6. Havaux, M.; Niyogi, K. K. The Violaxanthin Cycle Protects Plants from Photooxidative Damage by More than One Mechanism. *Proc. Natl. Acad. Sci. U.S.A.* **1999**, *96* (15), 8762–7.
- (5) Horton, P.; Johnson, M. P.; Perez-Bueno, M. L.; Kiss, A. Z.; Ruban, A. V. Photosynthetic Acclimation: Does the Dynamic Structure and Macro-Organisation of Photosystem II in Higher Plant Grana Membranes Regulate Light Harvesting States? *FEBS J.* **2008**, *275* (6), 1069–79. Walters, R. G. Towards an Understanding of Photosynthetic Acclimation. *J. Exp. Bot.* **2005**, *56* (411), 435–47. Ballottari, M.; Dall'Osto, L.; Morosinotto, T.; Bassi, R. Contrasting Behavior of Higher Plant Photosystem I and II Antenna Systems during Acclimation. *J. Biol. Chem.* **2007**, *282* (12), 8947–58. Bonente, G.; Pippa, S.; Castellano, S.; Bassi, R.; Ballottari, M. Acclimation of *Chlamydomonas reinhardtii* to Different Growth Irradiances. *J. Biol. Chem.* **2012**, *287* (8), 5833–47.
- (6) Demmig-Adams, B.; Adams, W. W.; Barker, D. H.; Logan, B. A.; Bowling, D. R.; Verhoeven, A. S. Using Chlorophyll Fluorescence to Assess the Fraction of Absorbed Light Allocated to Thermal Dissipation of Excess Excitation. *Physiol. Plant.* **1996**, *98* (2), 253–264.
- (7) Li, X. P.; Björkman, O.; Shih, C.; Grossman, A. R.; Rosenquist, M.; Jansson, S.; Niyogi, K. K. A Pigment-Binding Protein Essential for Regulation of Photosynthetic Light Harvesting. *Nature* **2000**, *403* (6768), 391–5.
- (8) Peers, G.; Truong, T. B.; Ostendorf, E.; Busch, A.; Elrad, D.; Grossman, A. R.; Hippler, M.; Niyogi, K. K. An Ancient Light-Harvesting Protein Is Critical for the Regulation of Algal Photosynthesis. *Nature* **2009**, *462* (7272), 518–21.
- (9) Dall'Osto, L.; Caffarri, S.; Bassi, R. A Mechanism of Non-photochemical Energy Dissipation, Independent from PsbS, Revealed by a Conformational Change in the Antenna Protein CP26. *Plant Cell* **2005**, *17* (4), 1217–32.
- (10) Ballottari, M.; Mozzo, M.; Croce, R.; Morosinotto, T.; Bassi, R. Occupancy and Functional Architecture of the Pigment Binding Sites of Photosystem II Antenna Complex Lhcb5. *J. Biol. Chem.* **2009**, *284* (12), 8103–13.
- (11) Betterle, N.; Ballottari, M.; Hienerwadel, R.; Dall'Osto, L.; Bassi, R. Dynamics of Zeaxanthin Binding to the Photosystem II Monomeric

Antenna Protein Lhcb6 (CP24) and Modulation of Its Photoprotection Properties. *Arch. Biochem. Biophys.* **2010**, *504* (1), 67–77.

(12) Dall'Osto, L.; Lico, C.; Alric, J.; Giuliano, G.; Havaux, M.; Bassi, R. Lutein Is Needed for Efficient Chlorophyll Triplet Quenching in the Major LHCII Antenna Complex of Higher Plants and Effective Photoprotection in Vivo under Strong Light. *BMC Plant Biol.* **2006**, *6*, 32.

(13) Groot, M. L.; Peterman, E. J.; van Kan, P. J.; van Stokkum, I. H.; Dekker, J. P.; van Grondelle, R. Temperature-Dependent Triplet and Fluorescence Quantum Yields of the Photosystem II Reaction Center Described in a Thermodynamic Model. *Biophys. J.* **1994**, *67* (1), 318–30.

(14) Peterman, E. J.; Dukker, F. M.; van Grondelle, R.; van Amerongen, H. Chlorophyll a and Carotenoid Triplet States in Light-Harvesting Complex II of Higher Plants. *Biophys. J.* **1995**, *69* (6), 2670–8.

(15) Peterman, E. J.; Gradinaru, C. C.; Calkoen, F.; Borst, J. C.; van Grondelle, R.; van Amerongen, H. Xanthophylls in Light-Harvesting Complex II of Higher Plants: Light Harvesting and Triplet Quenching. *Biochemistry* **1997**, *36* (40), 12208–15.

(16) Santabarbara, S.; Bordignon, E.; Jennings, R. C.; Carbonera, D. Chlorophyll Triplet States Associated with Photosystem II of Thylakoids. *Biochemistry* **2002**, *41* (25), 8184–94. Santabarbara, S.; Agostini, G.; Casazza, A. P.; Syme, C. D.; Heathcote, P.; Böhles, F.; Evans, M. C.; Jennings, R. C.; Carbonera, D. Chlorophyll Triplet States Associated with Photosystem I and Photosystem II in Thylakoids of the Green Alga *Chlamydomonas reinhardtii*. *Biochim. Biophys. Acta* **2007**, *1767* (1), 88–105.

(17) Dexter, D. L. A Theory of Sensitized Luminescence in Solids. *J. Chem. Phys.* **1953**, *21*, 15.

(18) Gall, A.; Berera, R.; Alexandre, M. T.; Pascal, A. A.; Bordes, L.; Mendes-Pinto, M. M.; Andrianambinintsoa, S.; Stoitchkova, K. V.; Marin, A.; Valkunas, L.; Horton, P.; Kennis, J. T.; van Grondelle, R.; Ruban, A.; Robert, B. Molecular Adaptation of Photoprotection: Triplet States in Light-Harvesting Proteins. *Biophys. J.* **2011**, *101* (4), 934–42.

(19) Mozzo, M.; Dall'Osto, L.; Hienerwadel, R.; Bassi, R.; Croce, R. Photoprotection in the Antenna Complexes of Photosystem II: Role of Individual Xanthophylls in Chlorophyll Triplet Quenching. *J. Biol. Chem.* **2008**, *283* (10), 6184–92.

(20) Passarini, F.; Wientjes, E.; Hienerwadel, R.; Croce, R. Molecular Basis of Light Harvesting and Photoprotection in CP24: Unique Features of the Most Recent Antenna Complex. *J. Biol. Chem.* **2009**, *284* (43), 29536–46.

(21) Liu, Z.; Yan, H.; Wang, K.; Kuang, T.; Zhang, J.; Gui, L.; An, X.; Chang, W. Crystal Structure of Spinach Major Light-Harvesting Complex at 2.72 Å Resolution. *Nature* **2004**, *428* (6980), 287–92.

(22) Pan, X.; Li, M.; Wan, T.; Wang, L.; Jia, C.; Hou, Z.; Zhao, X.; Zhang, J.; Chang, W. Structural Insights into Energy Regulation of Light-Harvesting Complex CP29 from Spinach. *Nat. Struct. Mol. Biol.* **2011**, *18* (3), 309–15.

(23) Caffarri, S.; Passarini, F.; Bassi, R.; Croce, R. A Specific Binding Site for Neoxanthin in the Monomeric Antenna Proteins CP26 and CP29 of Photosystem II. *FEBS Lett.* **2007**, *581* (24), 4704–10. Bonente, G.; Ballottari, M.; Truong, T. B.; Morosinotto, T.; Ahn, T. K.; Fleming, G. R.; Niyogi, K. K.; Bassi, R. Analysis of Lhcsr3, a Protein Essential for Feedback De-Excitation in the Green Alga *Chlamydomonas reinhardtii*. *PLoS Biol.* **2011**, *9* (1), e1000577.

(24) Caffarri, S.; Croce, R.; Breton, J.; Bassi, R. The Major Antenna Complex of Photosystem II Has a Xanthophyll Binding Site Not Involved in Light Harvesting. *J. Biol. Chem.* **2001**, *276* (38), 35924–33.

(25) Dall'osto, L.; Holt, N. E.; Kaligotla, S.; Fuciman, M.; Cazzaniga, S.; Carbonera, D.; Frank, H. A.; Alric, J.; Bassi, R. Zeaxanthin Protects Plant Photosynthesis by Modulating Chlorophyll Triplet Yield in Specific Light-Harvesting Antenna Subunits. *J. Biol. Chem.* **2012**, *287* (50), 41820–34. Jahns, P.; Wehner, A.; Paulsen, H.; Hobe, S. De-epoxidation of Violaxanthin after Reconstitution into Different Carotenoid Binding Sites of Light-Harvesting Complex II. *J. Biol. Chem.* **2001**, *276* (25), 22154–9.

(26) Ballottari, M.; Girardon, J.; Betterle, N.; Morosinotto, T.; Bassi, R. Identification of the Chromophores Involved in Aggregation-Dependent Energy Quenching of the Monomeric Photosystem II Antenna Protein Lhcb5. *J. Biol. Chem.* **2010**, *285* (36), 28309–21.

(27) Dall'osto, L.; Holt, N. E.; Kaligotla, S.; Fuciman, M.; Cazzaniga, S.; Carbonera, D.; Frank, H. A.; Alric, J.; Bassi, R. Zeaxanthin Protects Plant Photosynthesis by Modulating Chlorophyll Triplet Yield in Specific Light-harvesting Antenna Subunits. *J. Biol. Chem.* **2012**, *287* (50), 41820–34.

(28) Flors, C.; Fryer, M. J.; Waring, J.; Reeder, B.; Bechtold, U.; Mullineaux, P. M.; Nonell, S.; Wilson, M. T.; Baker, N. R. Imaging the Production of Singlet Oxygen in Vivo Using a New Fluorescent Sensor, Singlet Oxygen Sensor Green. *J. Exp. Bot.* **2006**, *57* (8), 1725–34.

(29) Frank, H. A.; Das, S. K.; Bautista, J. A.; Bruce, D.; Vasil'ev, S.; Crimi, M.; Croce, R.; Bassi, R. Photochemical Behavior of Xanthophylls in the Recombinant Photosystem II Antenna Complex, CP26. *Biochemistry* **2001**, *40* (5), 1220–5.

(30) Croce, R.; Canino, G.; Ros, F.; Bassi, R. Chromophore Organization in the Higher-Plant Photosystem II Antenna Protein CP26. *Biochemistry* **2002**, *41* (23), 7334–43.

(31) Bassi, R.; Pineau, B.; Dainese, P.; Marquardt, J. Carotenoid-Binding Proteins of Photosystem II. *Eur. J. Biochem.* **1993**, *212* (2), 297–303.

(32) Croce, R.; Remelli, R.; Varotto, C.; Breton, J.; Bassi, R. The Neoxanthin Binding Site of the Major Light Harvesting Complex (LHCII) from Higher Plants. *FEBS Lett.* **1999**, *456* (1), 1–6.

(33) Damjanović, A.; Ritz, T.; Schulten, K. Excitation Transfer in the Peridinin-Chlorophyll-Protein of *Amphidinium carterae*. *Biophys. J.* **2000**, *79* (4), 1695–705.

(34) Di Valentin, M.; Biasibetti, F.; Ceola, S.; Carbonera, D. Identification of the Sites of Chlorophyll Triplet Quenching in Relation to the Structure of LHC-II from Higher Plants. Evidence from EPR Spectroscopy. *J. Phys. Chem. B* **2009**, *113* (39), 13071–8.

(35) Dall'Osto, L.; Cazzaniga, S.; North, H.; Marion-Poll, A.; Bassi, R. The Arabidopsis aba4-1 Mutant Reveals a Specific Function for Neoxanthin in Protection against Photooxidative Stress. *Plant Cell* **2007**, *19* (3), 1048–64.

(36) Betterle, N.; Ballottari, M.; Zorzan, S.; de Bianchi, S.; Cazzaniga, S.; Dall'osto, L.; Morosinotto, T.; Bassi, R. Light-Induced Dissociation of an Antenna Hetero-oligomer Is Needed for Non-Photochemical Quenching Induction. *J. Biol. Chem.* **2009**, *284* (22), 15255–66.

(37) Giuffrè, E.; Cugini, D.; Croce, R.; Bassi, R. Reconstitution and Pigment-Binding Properties of Recombinant CP29. *Eur. J. Biochem.* **1996**, *238* (1), 112–20.

(38) de Bianchi, S.; Dall'Osto, L.; Tognon, G.; Morosinotto, T.; Bassi, R. Minor Antenna Proteins CP24 and CP26 Affect the Interactions between Photosystem II Subunits and the Electron Transport Rate in Grana Membranes of Arabidopsis. *Plant Cell* **2008**, *20* (4), 1012–28. de Bianchi, S.; Betterle, N.; Kouril, R.; Cazzaniga, S.; Boekema, E.; Bassi, R.; Dall'Osto, L. Arabidopsis Mutants Deleted in the Light-Harvesting Protein Lhcb4 Have a Disrupted Photosystem II Macrostructure and Are Defective in Photoprotection. *Plant Cell* **2011**, *23* (7), 2659–79. Croce, R.; van Amerongen, H. Light-Harvesting and Structural Organization of Photosystem II: from Individual Complexes to Thylakoid Membrane. *J. Photochem. Photobiol., B* **2011**, *104* (1–2), 142–53.

(39) Kühlbrandt, W.; Wang, D. N.; Fujiyoshi, Y. Atomic Model of Plant Light-Harvesting Complex by Electron Crystallography. *Nature* **1994**, *367* (6464), 614–21.

(40) Standfuss, J.; Terwisscha van Scheltinga, A. C.; Lamborghini, M.; Kühlbrandt, W. Mechanisms of Photoprotection and Non-photochemical Quenching in Pea Light-Harvesting Complex at 2.5 Å Resolution. *EMBO J.* **2005**, *24* (5), 919–28.

(41) Morosinotto, T.; Baronio, R.; Bassi, R. Dynamics of Chromophore Binding to Lhc Proteins in Vivo and in Vitro during Operation of the Xanthophyll Cycle. *J. Biol. Chem.* **2002**, *277* (40), 36913–20.



- (42) Formaggio, E.; Cinque, G.; Bassi, R. Functional Architecture of the Major Light-Harvesting Complex from Higher Plants. *J. Mol. Biol.* **2001**, *314* (5), 1157–66.
- (43) Ferroni, L.; Baldisserotto, C.; Giovanardi, M.; Pantaleoni, L.; Morosinotto, T.; Pancaldi, S. Revised Assignment of Room-Temperature Chlorophyll Fluorescence Emission Bands in Single Living Cells of *Chlamydomonas reinhardtii*. *J. Bioenerg. Biomembr.* **2011**, *43* (2), 163–73.
- (44) Marin, A.; Passarini, F.; Croce, R.; van Grondelle, R. Energy Transfer Pathways in the CP24 and CP26 Antenna Complexes of Higher Plant Photosystem II: a Comparative Study. *Biophys. J.* **2010**, *99* (12), 4056–65.
- (45) Marin, A.; Passarini, F.; van Stokkum, I. H.; van Grondelle, R.; Croce, R. Minor Complexes at Work: Light-Harvesting by Carotenoids in the Photosystem II Antenna Complexes CP24 and CP26. *Biophys. J.* **2011**, *100* (11), 2829–38. Schlau-Cohen, G. S.; Calhoun, T. R.; Ginsberg, N. S.; Read, E. L.; Ballottari, M.; Bassi, R.; van Grondelle, R.; Fleming, G. R. Pathways of Energy Flow in LHCII from Two-Dimensional Electronic Spectroscopy. *J. Phys. Chem. B* **2009**, *113* (46), 15352–63.
- (46) Croce, R.; Müller, M. G.; Bassi, R.; Holzwarth, A. R. Chlorophyll b to Chlorophyll a Energy Transfer Kinetics in the CP29 Antenna Complex: A Comparative Femtosecond Absorption Study between Native and Reconstituted Proteins. *Biophys. J.* **2003**, *84* (4), 2508–16.
- (47) Ahn, T. K.; Avenson, T. J.; Ballottari, M.; Cheng, Y. C.; Niyogi, K. K.; Bassi, R.; Fleming, G. R. Architecture of a Charge-Transfer State Regulating Light Harvesting in a Plant Antenna Protein. *Science* **2008**, *320* (5877), 794–7.
- (48) Mozzo, M.; Passarini, F.; Bassi, R.; van Amerongen, H.; Croce, R. Photoprotection in Higher Plants: The Putative Quenching Site Is Conserved in All Outer Light-Harvesting Complexes of Photosystem II. *Biochim. Biophys. Acta* **2008**, *1777* (10), 1263–7.